Communications in Physics, Vol. 32, No. 4 (2022), pp. 379-388
DOI: https://doi.org/10.15625/0868-3166/16787

STUDY OF CHARGE TRANSFER CONTRIBUTION TO SURFACE-ENHANCED RAMAN SCATTERING ACTIVITY OF Cu_2O NANO-OCTAHEDRAL SUBSTRATE

TRAN THU TRANG[1], VU XUAN HOA[1], PHAM THI THU HA[2,†], NGUYEN TRONG NGHIA[3] AND NGUYEN DAC DIEN[4]

[1]*Institute of Science and Technology, TNU-University of Sciences, Tan Thinh ward, Thai Nguyen city, Vietnam*

[2]*Faculty of Chemistry, TNU-University of Sciences, Tan Thinh ward, Thai Nguyen city, Vietnam*

[3]*Institute of Physics, Vietnam Academy of Science and Technology, 18 Hoang Quoc Viet, Cau Giay, Hanoi, Vietnam*

[4]*Faculty of Occupational Safety and Health, Vietnam Trade Union University, 169 Tay Son, Dong Da, Hanoi, Vietnam*

E-mail: †haptt@tnus.edu.vn

Received 9 December 2021; *Accepted for publication 10 June 2022*
Published 15 September 2022

Abstract. *In this study, a surface-enhanced Raman scattering (SERS) substrate based on an octahedral nanostructure of cuprous oxide (Cu_2O) was fabricated to probe methylene blue (MB) molecules. Cu_2O nanocrystals were synthesized by the solvothermal process using ethylene glycol, which plays both roles of reductant and organic solvent. The obtained Cu_2O nanocrystals have been characterized using scanning electron microscope (SEM), X-ray diffraction (XRD), energy-dispersive X-ray spectroscopy (EDX), Fourier-transform infrared spectroscopy (FTIR), and Raman spectroscopy. The SERS mechanism of the Cu_2O substrate was carefully investigated, and the results showed that both surface plasmon resonance and charge transfer phenomena contributed to SERS activity. Using a simple collection rule for SERS bands, the contributory portion of charge transfer process was estimated to be about 46%.*

Keywords: SERS; charge transfer contribution; octahedral Cu_2O nanocrystals.

Classification numbers: 78.30.-j.

I. INTRODUCTION

Surface-enhanced Raman scattering (SERS) has already been proven as an efficient analytical method for ultrasensitive detecting molecular species [1, 2]. SERS substrates based on metals

such as gold, silver, or copper have been demonstrated to be extremely effective in enhancing Raman scattering [3, 4]. Currently, semiconductor nanostructures have emerged as potential candidates for the SERS applications due to their interesting properties such as manageable bandgap, photoluminescence, good stability, and little degradation under light exposure [5, 6]. It should be noted that, in most cases of metal substrates, the predominant mechanism of SERS activity is electromagne(EM) enhancement, while the chemical enhancement exhibits a minor contribution. It is well-known that the EM mechanism is based on surface plasmon resonances (SPR), whereas the chemical enhancement mechanism results from charge transfer processes. One of the common threads in SERS research in semiconductor materials is the lack of a surface plasmon resonance of most laser excitations in the visible region. In fact, plasmons originating in the conduction band and the valence band of semiconductors are usually observed in the infrared and ultraviolet regions. Thus, the plasmon excitation energy is expected to range from 4 to 30 eV [6]. It is necessary to investigate the contribution of each mechanism to SERS enhancement. A better knowledge of SERS will help us improve the performance of SERS substrates [7]. However, quantifying the contribution of each mechanism to SERS behavior has not received much attention. The examination of SERS mechanism of semiconductor-based structures has been carried out on the structures such as the Cu/Cu_2O core-shell [8], Ag@Cu_2O core-shell [9], and Ag/PATP/ZnO sandwich [10].

It can be seen that cuprous oxide (Cu_2O) receives considerable attention due to its low cost, non-toxicity, abundant resources, and flexible optical bandgap [11]. Cu_2O is a p-type semiconductor with a relatively narrow direct bandgap of 1.8 – 2.5 eV, which corresponds to the energy of light in the visible region [12]. According to a comment in a review [5], the charge transfer effect is the most significant contribution to the SERS enhancement for Cu_2O-based substrates. Meanwhile, Malekfar and colleagues have recently demonstrated the dominance of surface plasmon resonances in the SERS enhancement mechanism of Cu/Cu_2O core-shell structures [8]. These findings suggest that the mechanism of SERS activity is probably highly dependent on the morphology of material surfaces.

In this work, we used the solvothermal route to prepare octahedral Cu_2O nanocrystals and then used the obtained Cu_2O nanocrystals as a SERS substrate to detect methylene blue (MB) molecules. The degree of charge transfer contribution to SERS activity of Cu_2O substrates was carefully evaluated using the SERS band selection rules. The results showed that both electromagnetic and charge transfer mechanisms exhibited equal contributions.

II. EXPERIMENT

II.1. Materials

Copper sulfate pentahydrate ($CuSO_4.5H_2O$, purity 99%), NaOH ($> 99\%$), ethylene glycol (CH_2OH-CH_2OH, $> 99\%$), and methylene blue were purchased from Sigma Aldrich Co., and used as received with no further purification.

II.2. Synthesis of Octahedral Cu_2O nanocrystals

Octahedral Cu_2O nanocrystals were synthesized by a solvothermal process. Six grams of NaOH powder were added to a glass flask containing 30 ml of deionized water and stirred until complete dissolve. After that, 120 ml of ethylene glycol (EG) and 12.5 g of $CuSO_4.5H_2O$ were added to the flask and vigorously stirred for 20 minutes at room temperature. The solution was then transferred to a Teflon-lined stainless steel autoclave container and heated at 180˚C for 10 hours.

After the solvothermal procedure, the product was cooled to room temperature before rinsing with deionized water and absolute ethanol to remove any excess solvent. The obtained sample was dried and stored in a desiccator. It should be noted that, unlike the standard procedure [13], our fabrication process did not use the reductant to reduce Cu^{2+} to Cu^{+}. EG plays both roles, organic solvent and reducing agent, which converted Cu^{2+} to Cu^{+}.

II.3. Characterization

The morphology of the obtained sample was investigated using a scanning electron microscope (SEM, Hitachi S4800) operating at 10 kV. The SEM technique employs a high-energy electron beam to scan the sample surface. The interaction between electrons and atoms on the surface of the sample will produce signals that provide information about surface topography. As a result, SEM can directly measure the size of nanostructures, as well as examine shape-related features. The X-ray diffraction pattern was obtained using Cu-K_α (0.154056 nm) radiation on an X-ray diffractometer (Bruker D8 Advance, Germany) with 2θ in the range of 30-80°. The chemical composition of samples was examined by energy-dispersive X-ray spectroscopy (EDX) mapping using the Hitachi SU 8020 at the elevated voltage of 200 kV. The spectrum was captured with a 0.5 nm probe diameter in 5 seconds. A JASCO 4600 (Japan) spectrophotometer was used to obtain an FTIR spectrum which provides the information of the functional group in octahedral Cu_2O nanocrystals. The UV-Vis reflection spectrum was recorded using a UV-Vis spectrophotometer (JASCO V770, Japan) with the wavelength in the range from 250 to 800 nm. The fluorescence spectrum was performed on an FLS1000 photoluminescence spectrometer. Raman spectra were recorded on Raman Horiba Zplora plus Raman microprobe (France) using a 532 nm excitation laser with the power of 3.2 mW and the collecting time of 10 s for each spectrum. The laser beam was focused on a circular point with a diameter of about 3.8 μm using a 100× objective lens. A silicon wafer with the Raman characteristic band at 520 cm^{-1} was used for spectrometer calibration. The SERS activity of the octahedral Cu_2O nanocrystal-based substrate was examined with methylene blue detection at a concentration of 10^{-4} M.

III. RESULTS AND DISCUSSION

III.1. Structural properties

Figure 1 shows SEM images of Cu_2O nanocrystals. The Cu_2O octahedral nanocrystals are well-defined, with a diameter of about 600 nm.

To characterize the structure of the octahedral Cu_2O nanostructure, the X-ray diffraction (XRD) pattern of the sample was examined, as shown in Fig. 2a. The spectra show that the sample contains two phases, cuprous oxide (JCPDS No. 05-0667) and copper (JCPDS No. 04-0836). More specifically, the cuprous oxide phase appears with the diffraction peaks at $2\theta = 29.6$, 36.5, 42.4, 61.6, 73.8, and 77.7 degrees, corresponding to the (110), (111), (200), and (220), (311), and (222) lattice planes, respectively (displayed as triangle symbols). There are also three diffraction peaks assigned to copper at 43.3, 50.45, and 74.12 degrees, which correspond to the (111), (200), and (220) planes (presented as square symbols). In addition, the EDX technique was used to confirm the sample's chemical composition (Fig. 2b). It can be seen that two elements have been found: Cu and O.

Furthermore, to identify the chemical bonds of the fabricated sample, Fourier transform infrared (FTIR) and Raman scattering experiments were implemented. Figure 3a describes the

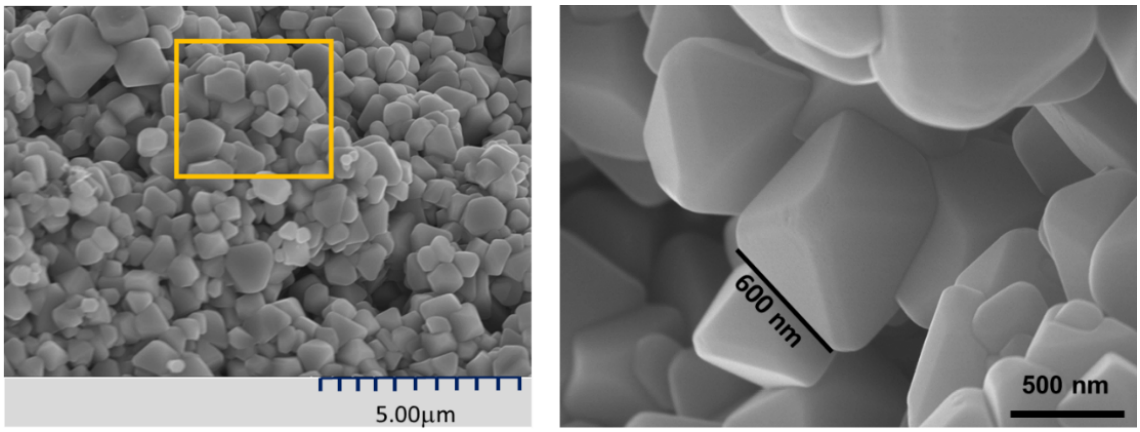

Fig. 1. SEM images of Cu_2O nanocrystals with different magnifications.

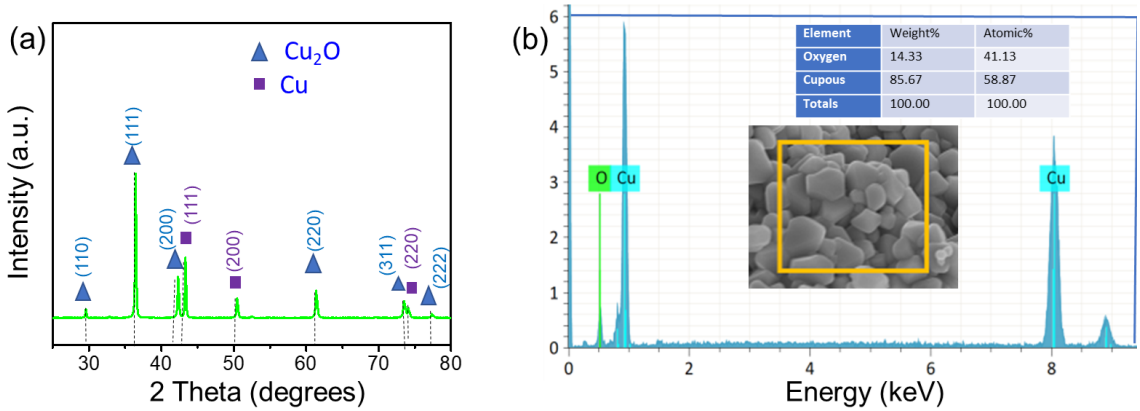

Fig. 2. (a) XRD pattern of Cu_2O nanocrystals and (b) EDX spectrum of Cu_2O nanocrystals for the area in the inset figure. In the XRD pattern, the diffraction peaks of Cu_2O are represented by triangle symbols, while square symbols mark the peaks of Cu.

FTIR spectrum of octahedral Cu_2O nanocrystals with an intense absorption peak at 628 cm^{-1} corresponding to the Cu_2O stretching mode [14]. The two broad bands at 3488 and 1632 cm^{-1} are ascribed to O–H stretching and bending modes of water molecules [15]. The band at 1386 cm^{-1} is attributed to the C–H vibration [15]. Two laser excitations at 532 nm and 785 nm were used to detect Raman spectra modes of Cu_2O nanocrystals. Using two excitation lasers will excite and identify Raman spectra modes of Cu_2O nanocrystals better than using one excitation laser. Therefore, the modes of the Cu_2O Raman spectra are well characterized with almost typical Raman modes that can be realized and listed as follows. It should be noted that the dominating Raman spectra of Cu_2O are caused by infrared-active modes or defect modes rather than Raman active modes. Precisely, the modes at about 89 cm^{-1} (T_{2u}) and 145 cm^{-1} (T_{1u} TO) correspond to optical absorption and active infrared modes, respectively [1, 3]. The peaks at 406 cm^{-1} and 630 cm^{-1} are assigned to multiphonon Raman scattering and T_{1u}TO modes of Cu_2O. The intense peak at

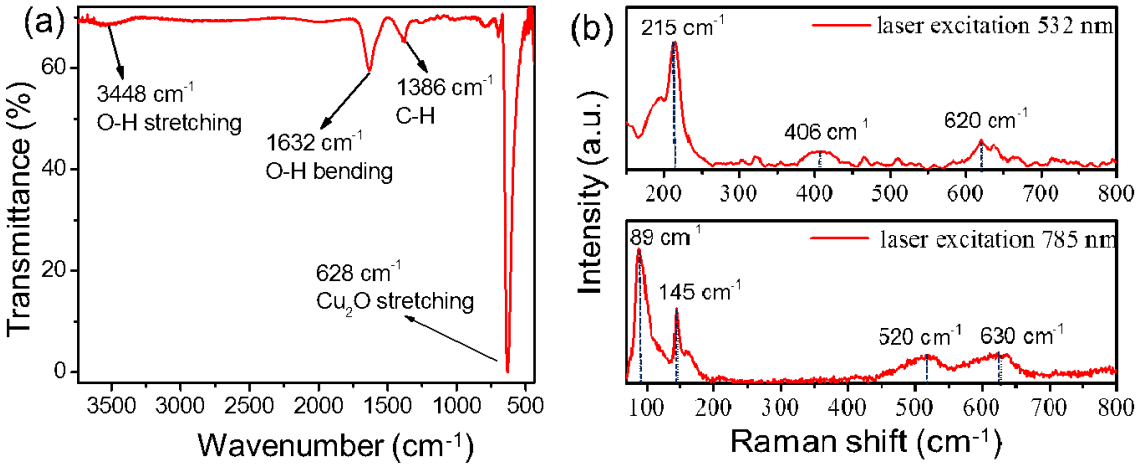

Fig. 3. (a) FTIR spectrum and (b) Raman spectra under two different laser excitations at 532 nm and 785 nm of octahedral Cu_2O nanocrystals.

215 cm^{-1} is attributed to the second-order overtone of Cu_2O, corresponding to the $2E_u$ mode [16]. The vicinity band of 520 cm^{-1} is the only Raman-active mode corresponding to the T_{2g} mode. Furthermore, the sharp mode at 215 cm^{-1}, which corresponds to the second-order overtone of Cu_2O, indicates that the Cu_2O nanocrystal has good structural quality [17].

III.2. Optical properties

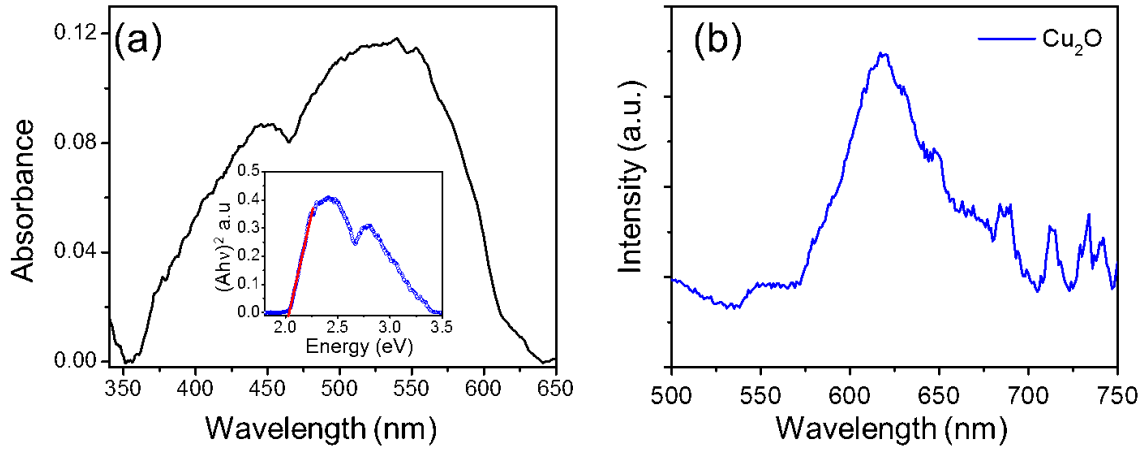

Fig. 4. (a) Absorption spectrum of Cu_2O nanocrystals along with plot of $(Ah\nu)^2$ versus $h\nu$ to determine bandgap value (in the inset of the figure); (b) Room temperature photoluminescence spectrum of Cu_2O nanocrystals in a 120 μl quart cell under 280 nm light excitation.

Figure 4 (a) shows the absorption spectrum of Cu_2O nanocrystal that was obtained using UV-Vis diffuse reflectance spectrometer. The spectrum of the sample with broadband from 450

nm to 550 nm is related to exciton transitions [18]. The bandgap of Cu_2O nanocrystals was obtained to be 2 eV by extrapolation according to the Tauc' law in the inset of Fig. 4(a). This observation shows good agreement with the optical characteristics of the Cu_2O structure [19, 20]. The photoluminescence spectrum of the sample is plotted in Fig. 4(b) with a band center at 630 nm, which is related to bound excitons [16, 21].

III.3. SERS study

SERS characteristics

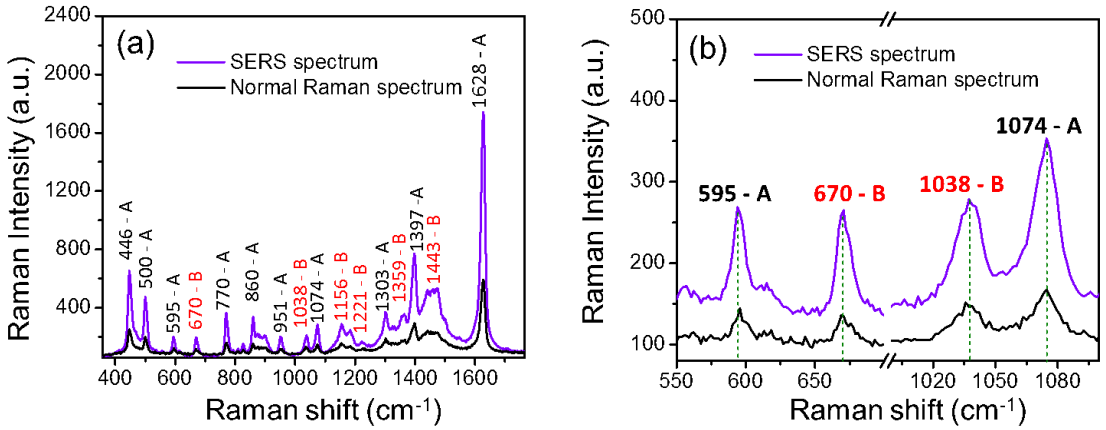

Fig. 5. (a) Normal Raman spectrum of MB (10^{-4} M) (black line) and SERS spectrum of MB (10^{-4} M) adsorbed on Cu_2O nanocrystals (violet line); (b) Zoom in the two wavenumber regions of these spectra, under 532 nm laser excitation.

In order to study the SERS behavior of octahedral Cu_2O nanocrystal surfaces, two different substrates, including MB (10^{-4}M) on bare glass and Cu_2O, which was spread on glass, were prepared for probing Raman signals of MB molecules. Fig. 5 displays the SERS spectrum of MB at a concentration of 10^{-4} M adsorbed on a Cu_2O substrate (violet line) in comparison with the normal Raman spectrum of MB (10^{-4} M) (black line). It is clear that the SERS spectrum based on the Cu_2O surface is significantly enhanced, and some wavenumber shifts are observed. These changes could be attributed to chemical enhancement, which is normally associated with the SERS effect from non-metal substrates [22]. The Raman spectrum of MB adsorbed on Cu_2O shows all the main recognized bands of MB. The modes at 446, 500, 595, 770, 860, 951, 1074, 1303, 1397, and 1625 cm^{-1} are totally symmetric vibrations, denoted as A modes. Whereas the modes at 670, 1038, 1156, 1221, 1359, and 1443 cm^{-1} are assigned as non-totally symmetric vibration bands, labeled as B modes [23, 24]. To estimate the activity of the SERS surface based on Cu_2O nanocrystals, the enhancement factor (EF) was evaluated for this SERS surface according to the equation [25]:

$$EF = \left(\frac{I_{\mathrm{SERS}}}{I_{\mathrm{nor}}}\right) \times \left(\frac{C_{\mathrm{nor}}}{C_{\mathrm{SERS}}}\right), \tag{1}$$

in which ISERS and Inor are the Raman intensities of MB molecules adsorbed on Cu_2O nanocrystals surface and normal Raman intensity of pure MB on the glass substrate, respectively. CSERS

and Cnor are the MB concentrations on the SERS substrate and the normal glass substrate, respectively. In our case, the analyte concentration is 10^{-4} M for both the SERS surface and the normal glass surface. The highest EF value has been obtained for the fingerprint band at 1628 cm^{-1} with a value of 3.2×10^3. This value is approximately ten orders of magnitude smaller than that in our previous work for ZnO microstructure surfaces [26]. It might be due to the natural mechanism of SERS activity on Cu_2O nanocrystal surfaces, which will be discussed in the next section.

SERS mechanism

As we all know, the contribution to the SERS enhancement includes two factors: i) electromagnetic enhancement, where surface plasmon resonance (SPR) is the main contribution; and ii) chemical enhancement, with the significant contribution originating from molecular resonance (or exciton resonance in the case of semiconductors) [13, 14]. It should be noted that the surface plasmon band of Cu_2O shows a broad and significant band from 360 nm to 660 nm (Fig. 4a), which overlaps with the laser excitation at 532 nm. As a result, it seems clear that the SPR effect contributes an important part to the SERS mechanism of Cu_2O nanocrystals in our experiment due to the resonance between the surface plasmon band of Cu_2O and the laser excitation at 532 nm. However, in order to obtain a full explanation of the SERS mechanism, the chemical enhancement factor will be discussed.

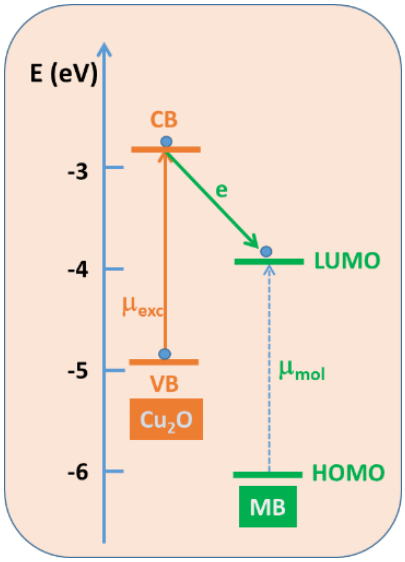

Fig. 6. Energy level diagram describing the SERS mechanism of MB adsorbed on a Cu_2O nanocrystal surface under laser excitation at 532 nm. Abbreviations: μ_{exc} = exciton resonance, μ_{mol} = molecular resonance, CB = conduction band, VB = valance band, HOMO = highest occupied molecular orbital, LUMO = lowest unoccupied molecular orbital.

As discussed in some reviews that have been published, charge transfer processes play an essential role in the chemical enhancement of SERS activity [5, 7]. Charge transfer processes can occur when the laser excitation coincides with molecular resonance or exciton resonance. As a result, the charge will be transferred from the valance band to the conduction band in the case of exciton resonance or from the highest occupied molecular orbital (HOMO) to the lowest unoccupied molecular orbital (LUMO) of the adsorbed molecule in the case of molecular resonance. Depending on the specific correlation between a given molecule and the SERS surface, one or the other process will take place.

For our case, HOMO and LUMO energy levels of MB molecules are at and eV, respectively [27], while the energy values of the conduction band and valance band of Cu_2O have been determined to be at and eV, respectively [28]. The excitation wavelength used in the SERS experiment is 532 nm (2.3 eV). It is relevant to the exciton resonance of Cu_2O nanocrystals with a bandgap of about 2 eV. Therefore, under the laser excitation, it is expected that the electron will

gain enough energy to jump from the valance band (VB) to the conduction band (CB) of Cu_2O and then move to the LUMO of MB molecules. This process is depicted in Fig. 6. It should be noted that the charge transferability of molecular resonance can be ignored because the energy of laser excitation does not coincide with the resonance energy of the MB molecule.

The above discussion helps us to understand the function of each process in the SERS activity of the Cu_2O substrate, which includes contributions from both electromagnetic and chemical enhancement. Keep in mind that normal Raman spectroscopy is similar for specific molecules. On the other hand, SERS spectroscopy depends on various resonant contributions, such as plasmon resonance and the charge transfer resonance. The relative degree of charge transfer contribution (ρ_{CT}) has been evaluated through the Herzberg-Teller-Surface selection rule using the following definition [29]:

$$\rho_{CT}(k) = \frac{I^k(CT) - I^k(SPR)}{I^k(CT) + I^0(SPR)}, \tag{2}$$

where k is an index used to identify individual lines in the SERS spectrum, I^k(CT) is the line (k) intensity in the SERS spectrum that represents the additional contribution of charge transfer to the SERS intensity caused by the SPR effect; I^k(SPR) is the intensity of the line (k) where only the SPR effect contributes to the intensity of SERS. In general, I^k(SPR) is relatively small. The other reference is a selected totally symmetric line, which was also measured with only SPR contributions, denoted as I^0(SPR).

According to the Herzberg-Teller-Surface selection rules, which govern the observed SERS spectrum intensity, the intensity enhancement of non-totally symmetric vibration bands can only be caused by the charge transfer effect. In contrast, totally symmetric modes tend to dominate the spectrum with only SPR contributions [7, 10, 29]. Thus, I^k(CT) can be determined by the intensity of the non-totally symmetric lines (INTSM). Meanwhile, I^0(SPR) is the intensity of the band only contributed by the SPR effect, and it also means that I^0(SPR) ascribes the intensity of a totally symmetric line, denoted as ITSM. Furthermore, due to the fact that excitation wavelength coincides with charge transfer resonance, the charge transfer contribution to SERS behavior I^k(CT) is more dominant than the contribution of I^k(SPR). Therefore, approximately, we take I^k(SPR) = 0. Thus, the formula (2) can be rewritten as:

$$\rho_{CT}(k) = \frac{I_{\mathrm{NTSM}}}{I_{\mathrm{NTSM}} + I_{\mathrm{TSM}}}. \tag{3}$$

Using the expression of which represents the intensity ratio in the SERS spectrum of non-totally symmetric mode of the analyte and its totally symmetric mode, the degree of charge transfer can be written as [7, 10]:

$$\rho_{CT} = \frac{R}{R+1}. \tag{4}$$

The detailed vibrational modes of MB have been well studied and indicated [23]. To choose bands as references for evaluating the degree of charge transfer contribution, the totally and non-totally symmetric modes should be fairly intense and well separated to suppress interference. As a result, two pairs of modes have been chosen. The first pair of modes is at 670 cm^{-1}, which is non-totally symmetric, and 595 cm^{-1}, which is totally symmetric. The second pair of modes is at 1038 cm^{-1} and 1074 cm^{-1}, corresponding to non-totally and totally symmetric bands, respectively. The mean degree of charge transfer contribution has been estimated to be around 46 $(\pm 2)\%$ for these modes

using Eq. (4) above. Such a value of ρ_{CT} demonstrates that the charge transfer mechanism is almost as significant as the EM mechanism in the SERS behavior of the Cu_2O nanocrystal substrate. Our findings are different from the previous observations that confirmed that the EM mechanism provided the primary contribution to the SERS signal enhancement [8]. This difference can be explained if we assume that the SERS activity of a substrate is dependent on its morphology [30].

IV. CONCLUSIONS

In summary, octahedral Cu_2O nanocrystals were fabricated by a solvothermal method and were used to detect MB molecules. The EF value for the MB fingerprint band at 1628 cm^{-1} was estimated at 3.2×10^3. The enhancement of Raman spectra of MB adsorbed on the Cu_2O nanocrystal surface was due to the combination of both electromagnetic enhancement and charge transfer effects, where the charge transfer effect accounted for approximately $46(\pm 2)\%$ of the total contribution. More specifically, the charge transfer effect occurred when there was a match between the photon energy of incident light and the bandgap energy of the Cu_2O nanocrystals.

ACKNOWLEDGMENT

This work was supported by Vietnam National Foundation for Science and Technology Development (NAFOSTED) under grant number 103.03-2020.32.

REFERENCES

[1] E. Le Ru, P. Etchegoin, *Principles of surface-enhanced Raman spectroscopy: and related plasmonic effects*, Elsevier, 2008.
[2] R. Aroca, *Surface-enhanced vibrational spectroscopy*, John Wiley & Sons, 2006.
[3] Z.-Q. Tian, B. Ren and D.-Y. Wu, *Surface-enhanced Raman scattering: From noble to transition metals and from rough surfaces to ordered nanostructures*, *J. Phys. Chem. B* **106** (2002) 9463.
[4] W. Li, P.H. Camargo, X. Lu and Y. Xia, *Dimers of silver nanospheres: Facile synthesis and their use as hot spots for surface-enhanced raman scattering*, *Nano -Lett.* **9** (2009) 485.
[5] I. Alessandri, J.R. Lombardi, *Enhanced Raman Scattering with Dielectrics*, *Chem Rev.* **116** (2016) 14921.
[6] J.R. Lombardi, R.L. Birke, *Theory of Surface-Enhanced Raman Scattering in Semiconductors*, *J. Phys. Chem. C* **118** (2014) 11120
[7] J.R. Lombardi, R.L. Birke, *A unified view of surface-enhanced Raman scattering Acc. Chem. Res.* **42** (2009) 734.
[8] H. Dizajghorbani Aghdam, S. Moemen Bellah, R. Malekfar, *Surface-enhanced Raman scattering studies of Cu/Cu_2O Core-shell NPs obtained by laser ablation*, textitSpectrochim. Acta-Part A Mol. Biomol. Spectrosc. **223** (2019) 117379.
[9] L. Chen, H. Sun, Y. Zhao, Y. Zhang, Y. Wang, Y. Liu, X. Zhang, Y. Jiang, Z. Hua, J. Yang, Plasmonic-induced SERS enhancement of shell-dependent Ag@Cu_2O core–shell nanoparticles, *RSC. Adv.* **7** (2017) 16553.
[10] A.P. Richter, J.R. Lombardi, B. Zhao, Size and wavelength dependence of the charge-transfer contributions to surface-enhanced Raman spectroscopy in Ag/PATP/ZnO junctions, *J. Phys. Chem. C* **114** (2010) 1610.
[11] N. Dasineh Khiavi, R. Katal, S. Kholghi Eshkalak, S. Masudy-Panah, S. Ramakrishna, H. Jiangyong, *Visible light driven heterojunction photocatalyst of CuO–Cu_2O thin films for photocatalytic degradation of organic pollutants*, *Nanomaterials* **9** (2019) 1011.
[12] F. Bayat and S. Sheibani, *Enhancement of photocatalytic activity of CuO-Cu_2O heterostructures through the controlled content of Cu_2O*, *Mater. Res. Bull* **145** (2022) 111561.
[13] S. S. Sawant, A. D. Bhagwat and C. M. Mahajan, *Synthesis of cuprous oxide (Cu_2O) nanoparticles–a review*, *J. Nano- Electron. Phys.* **8** (2016) 01035.
[14] A. Sahai, N. Goswami, S.D. Kaushik and S. Tripathi, *Cu/Cu_2O/CuO nanoparticles: Novel synthesis by exploding wire technique and extensive characterization*, *Appl. Surf. Sci.* **390** (2016) 974.

[15] D. Mardiansyah, T. Badloe, K. Triyana, M.Q. Mehmood, N. Raeis-Hosseini, Y. Lee, H. Sabarman, K. Kim and J. Rho, *Effect of temperature on the oxidation of Cu nanowires and development of an easy to produce, oxidation-resistant transparent conducting electrode using a PEDOT:PSS coating*, *Sci. Rep.* **8** (2018) 10639.

[16] H. Solache-Carranco, G. Juarez-Diaz, M. Galvan-Arellano, J. Martinez-Juarez and R. Pena-Sierra, *Raman scattering and photoluminescence studies on Cu_2O*, *2008 5th International Conference on Electrical Engineering, Computing Science and Automatic Contro* (2008) 421.

[17] B. K. Meyer, A. Polity, D. Reppin, M. Becker, P. Hering, B. Kramm, P.J. Klar, T. Sander, C. Reindl, C. Heiliger, M. Heinemann, C. Müller and C. Ronning, *Chapter Six -The Physics of Copper Oxide (Cu_2O)*, *Semiconductors and Semimetals*, *Semiconductors and Semimetals* **88** (2013) 201.

[18] T. Ito, T. Kawashima, H. Yamaguchi, T. Masumi and S. Adachi, *Optical properties of Cu_2O studied by spectroscopic ellipsometry*, *J. Phys. Soc. Jpn.* **67** (1998) 2125.

[19] S. Ishizuka, S. Kato, T. Maruyama and K. Akimoto, *Nitrogen doping into Cu_2O thin films deposited by reactive radio-frequency magnetron sputtering*, *Jpn. J. Appl. Phys.* **40** (2001) 2765.

[20] K. Sahu, A. Bisht, S.A. Khan, I. Sulania, R. Singhal, A. Pandey, S. Mohapatra, Thickness dependent optical, structural, morphological, photocatalytic and catalytic properties of radio frequency magnetron sputtered nanostructured Cu_2O–CuO thin films, *Ceram. Int.* **46** (2020) 14902.

[21] T. Ito and T. Masumi, *Detailed examination of relaxation processes of excitons in photoluminescence spectra of Cu_2O*, *J. Phys. Soc. Jpn.* **66** (1997) 2185-2193.

[22] L. Jin, G. She, X. Wang, L. Mu, W. Shi, *Enhancing the SERS performance of semiconductor nanostructures through a facile surface engineering strategy*, *Appl. Surf. Sci.* **320** (2014) 591.

[23] S. Dutta Roy, M. Ghosh, *J. Chowdhury, Adsorptive parameters and influence of hot geometries on the SER(R) S spectra of methylene blue molecules adsorbed on gold nanocolloidal particles*, *J. Raman Spectrosc.* **46** (2015) 451.

[24] S.D. Roy, P. Sett, M. Ghosh, J. Chowdhury, *Charge transfer mechanism and the adsorptive stance of methylene blue on gold nanocolloids: a vis-à-vis aftermath*, *J. Raman Spectrosc.* **48** (2017) 38.

[25] S. Kundu, W. Dai, Y. Chen, L. Ma, Y. Yue, A.M. Sinyukov, H. Liang, *Shape-selective catalysis and surface enhanced Raman scattering studies using Ag nanocubes, nanospheres and aggregated anisotropic nanostructures*, *J. Colloid Interface Sci.* **498** (2017) 248.

[26] T. T. H. Pham, X. H. Vu, T. T. Trang, N. X. Ca, N. D. Dien, P. Van Hai, N. T. Ha Lien, N. Trong Nghia, T. T. Kim Chi, *Enhance Raman scattering for probe methylene blue molecules adsorbed on ZnO microstructures due to charge transfer processes*, *Opt. Mater.* **120** (2021) 111460.

[27] Z. Zhang, Y. Yu and P. Wang, *Hierarchical top-porous/bottom-tubular TiO2 nanostructures decorated with Pd nanoparticles for efficient Photoelectrocatalytic decomposition of synergistic pollutants*, *ACS Appl. Mater. Interfaces* **4** (2012) 990.

[28] T. Oku, T. Yamada, K. Fujimoto and T. Akiyama, *Microstructures and photovoltaic properties of Zn(Al)O/Cu_2O-based solar cells prepared by spin-coating and electrodeposition*, *Coatings* **4** (2014) 203.

[29] J. R. Lombardi, R. L. Birke, *A unified approach to surface-enhanced Raman spectroscopy*, *J. Phys. Chem. C* **112** (2008) 5605.

[30] C. Qiu, Y. Bao, N. L. Netzer and C. Jiang, *Structure evolution and SERS activation of cuprous oxide microcrystals via chemical etching*, *J. Mater. Chem. A* **1** (2013) 8790.